Statefinder diagnostic and $w - w'$ analysis for interacting polytropic gas dark energy model.

M. Malekjani[1] *, A. Khodam-Mohammadi[1] †[1]

^{1}Department of Physics, Faculty of Science,
Bu-Ali Sina University, Hamedan 65178, Iran

arXiv:1201.0589v2 [gr-qc] 29 Apr 2012

Abstract

The interacting polytropic gas dark energy model is investigated from the viewpoint of statefinder diagnostic tool and $w - w'$ analysis. The dependency of the statefinder parameters on the parameter of the model as well as the interaction parameter between dark matter and dark energy is calculated. We show that different values of the parameters of model and different values of interaction parameter result different evolutionary trajectories in $s - r$ and $w - w'$ planes. The polytropic gas model of dark energy mimics the standard ΛCDM model at the early time.

* Email: malekjani@basu.ac.ir
† Email: khodam@basu.ac.ir

I. INTRODUCTION

Recent astronomical data obtained by SNe Ia [1], WMAP [2], SDSS [3] and X-ray [4] experiments suggest that our universe expands under an accelerated expansion. In the framework of standard cosmology, a dark energy component with negative pressure is responsible for this acceleration. A major puzzle of cosmology is the nature of dark energy and therefore many theoretical models have been proposed to interpret the behavior of dark energy. Although the earliest and simplest model is the Einstein's cosmological constant, but it suffers from tow deep theoretical problems namely the "fine-tuning" and "cosmic coincidence". The other models for dark energy scenario are the dynamical models in which the EoS parameter is time-varying. According to some analysis on the SNe Ia observational data, it has been shown that the time-varying dark energy models give a better fit compare with a cosmological constant [5]. The dynamical dark energy models are classified in tow different categories: (i) The scalar fields including quintessence [6], phantom [7], quintom [8], K-essence [9], tachyon [10], dilaton [11] and so forth. (ii) The interacting models of dark energy such as Chaplygin gas models [12, 13], braneworld models [14], holographic [15] and agegraphic [16] models. The interacting dark energy models have also been investigated in [17].

The holographic dark energy model comes from the holographic principle of quantum gravity [18] and the agegraphic model has been proposed based on the uncertainty relation of quantum mechanics together with general relativity [19]. Recent observational data gathered from the Abell Cluster A586 support the interaction between dark matter and dark energy [20]. However the strength of this interaction is not clearly identified [21].
Here in this work we focus on the polytropic gas model as a dark energy model to explain the cosmic acceleration. In stellar astrophysics, the polytropic gas model can explain the equation of state of degenerate white dwarfs, neutron stars and also the equation of state of main sequence stars [22]. The idea of dark energy with polytropic gas equation of state has been investigated by U. Mukhopadhyay and S. Ray in cosmology [23]. Recently, Karami et al. investigated the interaction between dark energy and dark matter in polytropic gas scenario, the phantom behavior of polytropic gas, reconstruction of $f(T)$- gravity from the polytropic gas and the correspondence between polytropic gas and agegraphic dark energy model [24–26]. The cosmological implications of polytropic gas dark energy model is also

discussed in [27]. The evolution of deceleration parameter in the context of polytropic gas dark energy model represents the decelerated expansion at the early universe and accelerated phase later. Depending on the parameters of the model, the polytropic gas can achieve a quintessence regime. The potential and the dynamics of K-essence, dilaton and tachyon fields according to the evolution of polytropic gas model is also investigated in [27].

The polytropic gas is a phenomenological model of dark energy. In a phenomenological model, the pressure p is a function of energy density ρ, i.e., $p = -\rho - f(\rho)$ [28]. For $f(\rho) = 0$, the equation of state of phenomenological models can cross $w = -1$, i.e., the cosmological constant model. Nojiri, et al. investigated four types singularities for some illustrative examples of phenomenological models [28]. The polytropic gas model has a type III. singularity in which the singularity takes place at a characteristic scale factor a_s.

Since many theoretical dark energy models have been proposed to explain the accelerated expansion of the universe, therefore a sensitive test which can discriminate between these models is required. The Hubble parameter, $H = \dot{a}/a$, (first time derivative) and the deceleration parameter $q = -\ddot{a}/aH^2$ (second time derivative) are the geometrical parameters to describe the expansion history of the universe. Since $\dot{a} > 0$, hence $H > 0$ means the expansion of the universe. Also $\ddot{a} > 0$, i.e. $q < 0$, indicates the accelerated expansion of the universe. Since the various dark energy models give $H > 0$, $q < 0$ at the percent time, hence the Hubble parameter and deceleration parameter can not discriminate dark energy models. For this aim we need a higher order of time derivative of scale factor. Sahni et al. [29] and Alam et al. [30], by using the third time derivative of scale factor, introduced the statefinder pair {s,r} in order to remove the degeneracy of H and q at the present time. The statefinder pair has been given by

$$r = \frac{\dddot{a}}{aH^3}, s = \frac{r-1}{3(q-1/2)} \tag{1}$$

Depending the statefinder diagnostic tool on the scale factor indicates that the statefinder parameters are geometrical. Up to now, the various dark energy models have been studied from the viewpoint of statefinder diagnostic. The various dark energy models have different evolutionary trajectories in {s, r} plane, therefore the statefinder tool can discriminate these models. The well known ΛCDM model is related to the fixed point {s=0,r=1} in the $s - r$ plane [29]. The other dynamical dark energy models that have been investigated by statefinder diagnostic tool are:

the quintessence DE model [29, 30] , the interacting quintessence models [31, 32], the holographic dark energy models [33, 34] , the holographic dark energy model in non-flat universe [35], the phantom model [36], the tachyon [37], the generalized chaplygin gas model [38], the interacting new agegraphic DE model in flat and non-flat universe [39, 40], the agegraphic dark energy model with and without interaction in flat and non-flat universe [41, 42] are analyzed through the statefinder diagnostic tool. Recently, the statefinder parameters have been investigated by considering the variable gravitational constant G [43].

In addition to statefinder diagnostic, the other analysis to discriminate between dark energy models is $w - w'$ analysis that have been used widely in the papers [40–42, 44–53]. In this work we investigate the interacting polytropic gas model by statefinder diagnostic tool and $w - w'$ analysis. We introduce the interacting polytropic gas dark energy model in sect. II. The numerical results is presented in sect. III. We conclude in sect.IV.

II. INTERACTING POLYTROPIC GAS DARK ENERGY MODEL

In this section we give a brief review of the polytropic gas model for dark energy scenario. For more details and discussion see [27]. The equation of state (EoS) of polytropic gas is given by

$$p_\Lambda = K\rho_\Lambda^{1+\frac{1}{n}}, \tag{2}$$

where K and n are the polytropic constant and polytropic index, respectively [22].

In the non-flat FRW universe including dark energy and dark matter components, the Friedmann equation is given by

$$H^2 + \frac{k}{a^2} = \frac{1}{3M_p^2}(\rho_m + \rho_\Lambda) \tag{3}$$

where H is the Hubble parameter, M_p is the reduced Planck mass and $k = 1, 0, -1$ is a curvature parameter corresponding to the closed, flat and open universe, respectively. ρ_m and ρ_Λ are the energy densities of dark matter and dark energy, respectively.

The dimensionless energy densities are defined as

$$\Omega_m = \frac{\rho_m}{\rho_c} = \frac{\rho_m}{3M_p^2 H^2}, \quad \Omega_\Lambda = \frac{\rho_\Lambda}{\rho_c} = \frac{\rho_\Lambda}{3M_p^2 H^2} \quad \Omega_k = \frac{k}{a^2 H^2} \tag{4}$$

Therefore the Friedmann equation (3) can be written as

$$\Omega_m + \Omega_\Lambda = 1 + \Omega_k. \tag{5}$$

In a universe dominated by interacting dark energy and dark matter, the total energy density, $\rho = \rho_m + \rho_\Lambda$, satisfies a conservation equation

$$\dot{\rho} + 3H(\rho + p) = 0 \tag{6}$$

However, by considering the interaction between dark energy and dark matter, the energy density of dark energy and dark matter does not conserve separately and in this case the conservation equations for each component are given by

$$\dot{\rho_m} + 3H\rho_m = Q, \tag{7}$$

$$\dot{\rho_\Lambda} + 3H(\rho_\Lambda + p_\Lambda) = -Q, \tag{8}$$

where Q represents the interaction between dark components and can be given as one of the following forms [54]

$$Q = \begin{cases} 3\alpha H \rho_\Lambda \\ 3\beta H \rho_m \\ 3\gamma H(\rho_\Lambda + \rho_m) \end{cases} \tag{9}$$

where α, β and γ are the dimensionless constants. The Hubble parameter H in the Q-terms is considered for mathematical simplicity. The interaction parameter Q indicates the decay rate of dark energy to the dark matter component. The interaction between dark energy and dark matter is also studied in [55]. Here same as our previous works, for mathematical simplicity, we consider the first form of interaction parameter Q [27, 40, 42]. Using Eq.(2), the integration of continuity equation for interacting dark energy component, i.e. Eq.(8), gives

$$\rho_\Lambda = \left(\frac{1}{Ba^{\frac{3(1+\alpha)}{n}} - \widetilde{K}} \right)^n, \tag{10}$$

where B is the integration constant, $\widetilde{K} = \frac{K}{1+\alpha}$ and a is the scale factor. A positive energy density for any value of n is achieved when $Ba^{3(1+\alpha)/n} > \widetilde{K}$. In the case of even n, we have positive energy density for any condition of $\widetilde{K}$. The phantom behavior of interacting polytropic gas dark energy has been studied in [25]. In the case of $Ba^{3(1+\alpha)/n} = \widetilde{K}$, we have $\rho \to \infty$ and the polytropic gas has a finite-time singularity at $a_c = (\widetilde{K}/B)^{n/3(1+\alpha)}$. This type of singularity, in which at a characteristic scale factor a_s, the energy density $\rho \to \infty$ and the pressure density $|p| \to \infty$, has been indicated by type III singularity [28]. Substituting $Q = 3\alpha H \rho_\Lambda$ in (8) obtains

$$\dot{\rho_\Lambda} + 3H(1 + \alpha + w_\Lambda)\rho_\Lambda = 0, \tag{11}$$

Taking the derivative of Eq.(10) with respect to time, one can obtain

$$\dot{\rho}_\Lambda = -3BH(1+\alpha)a^{\frac{3(1+\alpha)}{n}}\rho_\Lambda^{1+\frac{1}{n}} \tag{12}$$

Substituting Eq.(12) in (11) and using Eq.(10), we can obtain the EoS parameter of interacting polytropic gas as

$$w_\Lambda = -1 - \frac{a^{\frac{3(1+\alpha)}{n}}}{c - a^{\frac{3(1+\alpha)}{n}}} - \alpha \tag{13}$$

where $c = \widetilde{K}/B$. We see that the interacting polytropic gas model behaves as a phantom model, i.e. $w_\Lambda < -1$, when $c > a^{3(1+\alpha)/n}$. It is also clear to see that at the early time $(a \to 0)$ and the absence of interaction between dark matter and dark energy $(\alpha = 0)$, the polytropic gas mimics the constant, i.e. $w_\Lambda \to -1$. The evolution of EoS parameter can be obtained by differentiating of (13) as follows

$$w_\Lambda' = -\frac{3(1+\alpha)ca^{\frac{3(1+\alpha)}{n}}}{n(c - a^{\frac{3(1+\alpha)}{n}})^2} \tag{14}$$

where prime denotes the derivative with respect to $x = \ln a$. Using Eqs.(10) and (4) the density parameter of interacting polytropic gas is given by

$$\Omega_\Lambda = \frac{(Ba^{\frac{3(1+\alpha)}{n}} - \widetilde{K})^{-n}}{3M_p^2 H^2} \tag{15}$$

Taking the time derivative of Eq.(15) and using $\Omega' = \dot{\Omega}/H$, yields

$$\Omega_\Lambda' = -\Omega_\Lambda\left(\frac{3(1+\alpha)a^{\frac{3(1+\alpha)}{n}}}{a^{\frac{3(1+\alpha)}{n}} - c} + 2\frac{\dot{H}}{H^2}\right) \tag{16}$$

Taking the time derivative of Friedmann equation (3) and using Eqs.(10), (5), (7), (15) and $Q = 3\alpha H\rho_\Lambda$, one can find that

$$\frac{\dot{H}}{H^2} = -\frac{3}{2}\left[\Omega_\Lambda\frac{c(1+\alpha)}{a^{\frac{3(1+\alpha)}{n}} - c} + 1 + \frac{\Omega_k}{3}\right] \tag{17}$$

Substituting this relation into Eq.(16), we obtain the evolutionary equation for energy density parameter of interacting polytropic gas as:

$$\Omega_\Lambda' = -3\Omega_\Lambda\left[\frac{c}{a^{\frac{3(1+\alpha)}{n}} - c}(1 - \Omega_\Lambda) + \alpha\frac{a^{\frac{3(1+\alpha)}{n}} - c\Omega_\Lambda}{a^{\frac{3(1+\alpha)}{n}} - c} - \frac{\Omega_k}{3}\right], \tag{18}$$

The evolution of density parameter Ω_Λ has been discussed in [27]. It has been shown that the polytropic gas dark energy model can describe the matter dominated universe at the

early time, $\Omega_\Lambda \to 0$, and dark energy universe at the late time, $\Omega_\Lambda \to 1$, see Fig.(2) of [27]. The deceleration parameter is given by

$$q = -\frac{\ddot{a}}{aH^2} = -1 - \frac{\dot{H}}{H^2} \tag{19}$$

Substituting (17) in (19), the deceleration parameter can be obtained as

$$q = -1 + \frac{3}{2}\left[\Omega_\Lambda \frac{c(1+\alpha)}{a^{\frac{3(1+\alpha)}{n}} - c} + 1 + \frac{\Omega_k}{3}\right] \tag{20}$$

The evolution of q for interacting polytropic gas model has also been presented in [27]. At the early time the universe has a decelerated expansion, $q > 0$, and enters into the accelerated phase later, $q < 0$, see Fig.(3) of [27].

Using (13), (17) and (20), we have

$$\frac{\ddot{H}}{H^3} = -\frac{9}{2}\Omega_\Lambda(1+\alpha)(\alpha+w_\Lambda)[(1+\alpha)(-w_\Lambda+\Omega_\Lambda\alpha+\Omega_\Lambda w_\Lambda) - \alpha(\alpha+2)]$$
$$-\frac{3}{2}\Omega_\Lambda(1+\alpha)w_\Lambda' + \frac{9}{2}[\Omega_\Lambda(1+\alpha)(\alpha+w_\Lambda)+1]^2 \tag{21}$$

At what follows, we derive the statefinder parameters (s, r) for polytropic gas model in the interacting spatially flat universe. Using the definition of statefinder parameters in (1), one can obtain

$$r = \frac{\dddot{a}}{aH^3} = \frac{\ddot{H}}{H^3} - 3q - 2 \tag{22}$$

Inserting (20) and (21) in (22) and using (16) we have

$$r = 1 + \frac{3}{2}\Omega_\Lambda(1+\alpha)[3(1+\alpha)(\alpha+w_\Lambda)(1+\alpha+w_\Lambda) - w_\Lambda'] \tag{23}$$

Inserting (20) and (23) in (1), the parameter s for interacting polytropic gas is obtained as

$$s = \frac{2}{3}\frac{3\alpha(\alpha+1)^2 + 3\alpha w_\Lambda(2\alpha+w_\Lambda+3) + 3w_\Lambda(1+w_\Lambda) - w_\Lambda'}{\alpha+w_\Lambda} \tag{24}$$

In the limiting case of $w_\Lambda = -1$, it is obvious $w_\Lambda' = 0$ and in the absence of interaction between dark matter and dark energy, i.e. $\alpha = 0$, the statefinder parameters reduce to $\{s = 0, r = 1\}$ which is coincide to the location of standard ΛCDM model in $s - r$ plane.

III. NUMERICAL RESULTS

In the present section we give the numerically description of the evolutionary trajectories of the statefinder parameters in $s - r$ plane for interacting polytropic gas dark energy

model in the flat universe. We also perform the $w - w'$ analysis for this model. Here we set $\Omega_m^0 = 0.3$ and $\Omega_\Lambda^0 = 0.7$ for the density parameters of dark matter and dark energy at the present time, respectively.

A. Statefinder diagnostic

The statefinder pair $\{s, r\}$ in this model is given by (23) and (24). One can easily see the dependency of the $\{s, r\}$ on the EoS parameter , w, as well as the interaction parameter α in (23) and (24). In the limiting case of non-interacting polytropic gas ($\alpha = 0$), from (13) we see that at the early time ($a \to 0$) the EoS parameter $w_\Lambda \to -1$. From (14), we also have $w_\Lambda' \to 0$. From (23) and (24) we see that at the early time the statefinder parameters for non-interacting flat universe are ($s = 0, r = 1$) which is coincide to the location of spatially flat ΛCDM model in the $s - r$ plane. Hence, the polytropic gas model mimics the ΛCDM model at the early time.

In Fig.(1), the evolutionary trajectories of interacting polytropic gas model is plotted for different values of interaction parameter α. Here we fix the parameters of the model as $c = 2, n = 4$. The standard ΛCDM fixed point is indicated by star symbol in this diagram. The colored circles on the curves show the present values of statefindr pair $\{s_0, r_0\}$. Different values of α result different evolutionary trajectories in $s - r$ plane. Hence the interaction parameter can influence on the evolutionary trajectory of polytropic gas model in $s - r$ plane. For larger value of α, the present value s_0 decreases and the present value r_0 increases. The distance of the point (s_0, r_0) form the ΛCDM fixed point (i.e. $s = 0, r = 1$) becomes larger by increasing the interaction parameter α. While the universe expands, the evolutionary trajectory of interacting polytropic gas dark energy model evolves from the ΛCDM at the early time, then r increases and s decreases. The present value $\{s_0, r_0\}$ are valuable, if it can be extracted from the future data of SNAP (SuperNova Acceleration Probe) experiments. Therefore, the statefinder diagnostic tool with future SNAP observation are useful to discriminate between various dark energy models.

In Fig.(2), the evolutionary trajectories for interacting polytropic gas are plotted for different values of the parameters of the model. Here we fix the interaction parameter as $\alpha = 0$. In left panel, the parameter n is fixed and the parameter c is varied. Different values

of c gives the different evolutionary trajectories in $s - r$ plane. Therefore the parameter c of the model can affect on the evolutionary trajectories in $s - r$ plane. Like Fig.(1), the present value of statefinder pair, i.e. $\{s_0, r_0\}$ is indicated by colore circles on the curves. For larger values of c, r_0 decreases and s_0 increases. The distance of the point (s_0, r_0) to the location of standard ΛCDM fixed point becomes shorter for larger value of c. In right panel the parameter c is fixed and the parameter n is varied. Same as left panel, the interaction parameter is fixed to $\alpha = 0$. Here we also see that different values of n gives different evolutionary trajectories in $s - r$ plane. For larger values of n, we see r_0 decreases and s_0 increases. Here we see that, same as parameter c, the distance of the point (s_0, r_0) to the location of standard ΛCDM fixed point becomes shorter for larger value of n.

B. $w_\Lambda - w_\Lambda'$ analysis

In addition to the statefinder diagnostic, another analysis to discriminate various models of dark energy is $w - w_\Lambda'$ analysis. Here we apply this analysis for interacting polytropic gas dark energy model. In this analysis the standard ΛCDM model corresponds to $\{w_\Lambda = -1, w_\Lambda' = 0\}$. The evolution of w_Λ and w_Λ' are given by (13) and (14), respectively. In Fig.(3), the evolutionary trajectories of interacting polytropic gas dark energy for different values of interaction parameter are shown in $w_\Lambda - w_\Lambda'$ plane. Here we fix the parameter of the polytropic model as $c = 2$ and $n = 4$. One can see the different values of α result different trajectories in $w_\Lambda - w_\Lambda'$ plane. The present value $w_\Lambda^0 - w_\Lambda'^0$ is dependent on the interaction parameter. Larger value of α obtains smaller values of w_Λ^0 and $w_\Lambda'^0$.

In Fig.(4), the evolutionary trajectories are plotted in the absence of interaction parameter, i.e. $\alpha = 0$. Here we perform the $w_\Lambda - w_\Lambda'$ analysis for different values of the parameters of model. In left panel the parameter n is fixed and in the right panel the parameter c is fixed. In these diagrams, by expanding the universe, the evolutionary trajectories start from the fixed point $w_\Lambda = -1, w_\Lambda' = 0$ (i.e. the location of ΛCDM fixed point). In left panel, one can see that the parameter c can only affect the present value $w_\Lambda^0 - w_\Lambda'^0$. Different values of c result the same evolutionary trajectory in $w_\Lambda - w_\Lambda'$ plane. The distance of the present value $w_\Lambda^0 - w_\Lambda'^0$ to the location of ΛCDM fixed point (i.e. $\{w_\Lambda = -1, w_\Lambda' = 0\}$) is shorter for larger value of c. In right panel we have different evolutionary trajectories in $w_\Lambda - w_\Lambda'$

plane for different values of n. The parameter w'^0_Λ increases for larger value of n. Like left panel, the distance of the present value $w^0_\Lambda - w'^0_\Lambda$ to the location of ΛCDM model is shorter for larger value of n.

IV. CONCLUSION

Since many dynamical dark energy models have been proposed to interpret the cosmic acceleration, the statefinder diagnostic tool based on third time derivative of scale factor is given to discriminate between them. The statefinder diagnostic combined with future SNAP observation can be useful to discriminate between various dark energy models. Here we studied the statefinder diagnostic tool for interacting polytropic gas model in spatially flat universe. We derive the statefinder parameters s and r in this model and investigate the dependency of the evolutionary trajectories in $s - r$ plane on the parameters of the model as well as the interaction parameter between dark matter and dark energy. We obtained the present value $\{s_0, r_0\}$ of this model and studied the dependency of $\{s_0, r_0\}$ on the parameters of the model and interaction parameter. By expanding the universe, the evolutionary trajectories start from the ΛCDM fixed point then r increases and s decreases. For smaller value of interaction parameter α, the distance of $\{s_0, r_0\}$ from the location of ΛCDM fixed point becomes shorter. Also the larger values of c and n result the shorter distance from the ΛCDM fixed point. The behavior of interacting polytropic gas in $s - r$ plane is similar with the new holographic dark energy model (see Fig.(4) of [56]). For both models, by expanding the universe, r increases and s decreases. Finally we studied the $w - w'$ analysis for this model. We showed that the evolutionary trajectories in $w - w'$ plane is dependent on the parameters of the model and also the interaction parameter α. While the universe expands, the trajectories starts from the location of ΛCDM fixed point (i.e. $\{w_\Lambda = -1, w'_\Lambda = 0\}$). Hence the polytropic gas model mimics the standard ΛCDM fixed point at the early time. The agegraphic dark energy model also mimics the ΛCDM model at the early time [40, 41]. At future the high-precision SNAP-type experiment can be useful to determine the statefinder parameters precisely and consequently single out the right dark energy models.
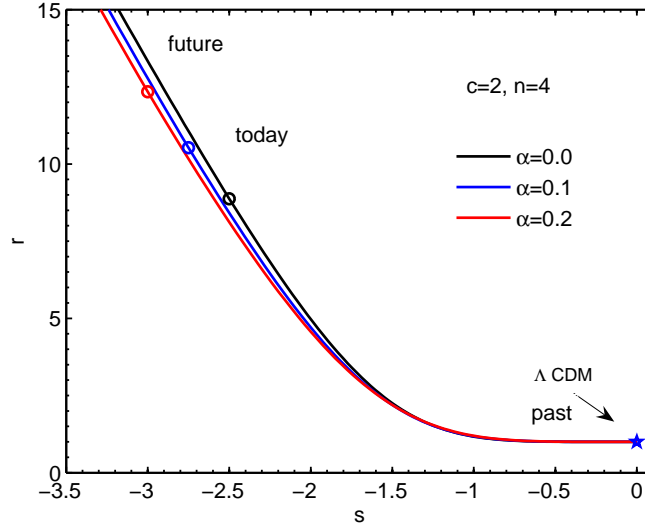
FIG. 1: The evolutionary trajectories for interacting polytropic gas model in $s-r$ plane for different values of interaction parameter α. The black curve indicates the non-interacting case and the blue and red curves represent $\alpha = 0.1, 0.2$, respectively. The circles on the curves show the present value of the statefinder pair $\{s_0, r_0\}$. The star symbol is related to the location of standard ΛCDM model in $s-r$ plane. The parameters of the model are chosen as $c = 2, n = 4$.
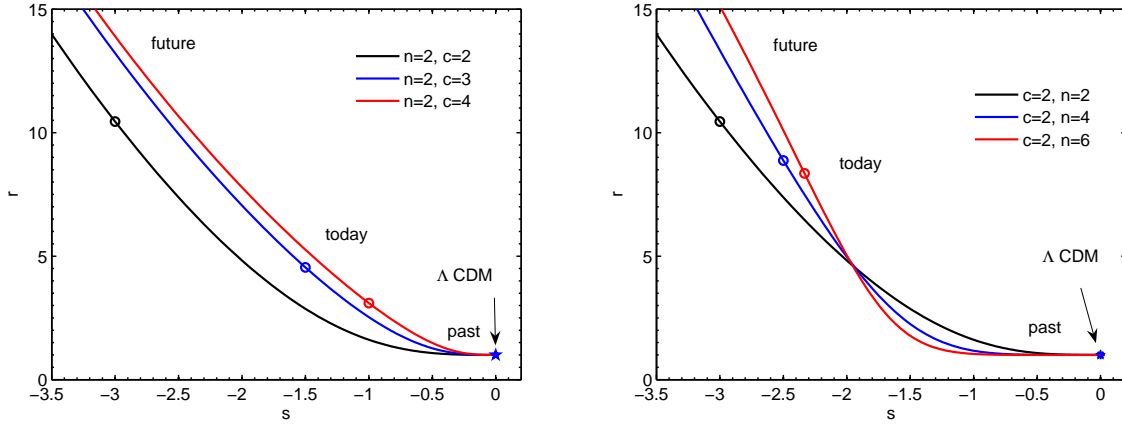
FIG. 2: The evolutionary trajectories for polytropic gas model in $s-r$ plane for different illustrative values of parameters c and n. Here we choose the interaction parameter as $\alpha = 0$. In left panel the parameter n is fixed and the parameter c is varied as $c = 2$(black curve), $c = 3$ (blue curve), $c = 4$ (red curve). In right panel the parameter c is fixed and the parameter n is varied as $n = 2$ (black curve), $n = 4$ (blue curve) and $n = 6$ (red curve). The circles on the curves show the present value of the statefinder pair $\{s_0, r_0\}$. The star symbol is related to the location of standard ΛCDM model in $s - r$ plane.
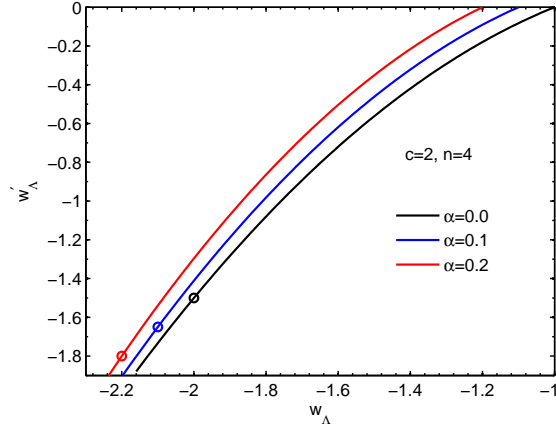
FIG. 3: The evolutionary trajectories for interacting polytropic gas model in $w_\Lambda - w'_\Lambda$ plane for different values of interaction parameter α. The black curve shows the non-interacting case and the blue and red curves indicate $\alpha = 0.1, 0.2$, respectively. The colored circles on the curves show the present value $w_\Lambda^0 - w_\Lambda'^0$. The parameters of the model are chosen as $c = 2, n = 4$.
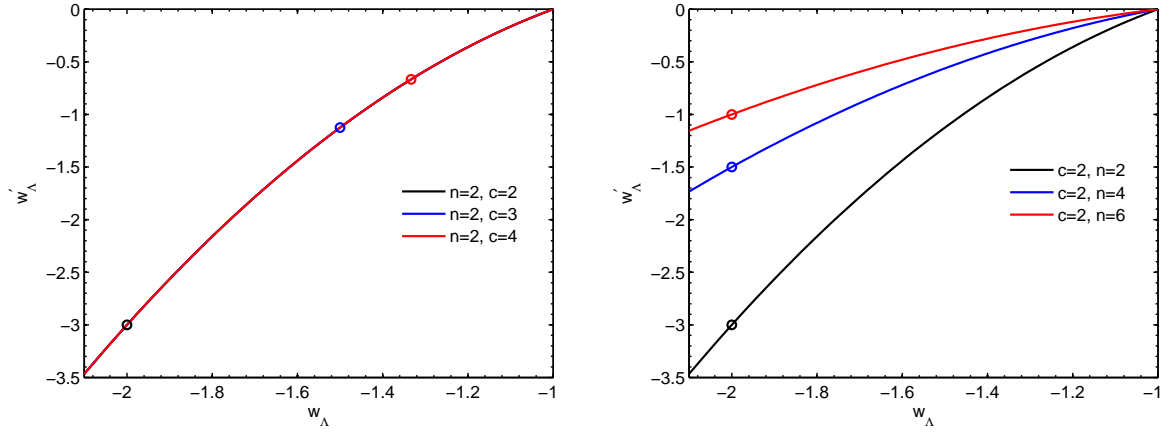
FIG. 4: The evolutionary trajectories for polytropic gas model in $w_\Lambda - w'_\Lambda$ plane for different illustrative values of parameters c and n. Here the interaction parameter is chosen as $\alpha = 0$. In left panel the parameter n is fixed and the parameter c is varied as $c = 2$(black curve), $c = 3$ (blue curve), $c = 4$ (red curve). In right panel the parameter c is fixed and the parameter n is varied as $n = 2$ (black curve), $n = 4$ (blue curve) and $n = 6$ (red curve).

[1] S. Perlmutter et al., Astrophys. J. **517**, 565 (1999).

[2] C. L. Bennett et al., Astrophys. J. Suppl. **148**, 1 (2003).

[3] M. Tegmark et al., Phys. Rev. D **69**, 103501 (2004).

[4] S. W. Allen, et al., Mon. Not. Roy. Astron. Soc. **353**, 457 (2004).

[5] U. Alam, V. Sahni and A. A. Starobinsky, JCAP **0406** (2004) 008; D. Huterer and A. Cooray, Phys. Rev. D **71** (2005) 023506; Y.G. Gong, Int. J. Mod. Phys. D 14 (2005) 599; Y.G. Gong, Class. Quantum Grav. **22** (2005) 2121; Yun Wang and M. Tegmark, Phys. Rev. D **71** (2005) 103513; Yun-gui Gong and Yuan-Zhong Zhang, Phys. Rev. D **72** (2005) 043518.

[6] C. Wetterich, Nucl. Phys. B **302**, 668 (1988);

B. Ratra, J. Peebles, Phys. Rev. D **37**, 321 (1988).

[7] R. R. Caldwell, Phys. Lett. B **545**, 23 (2002);

S. Nojiri, S.D. Odintsov, Phys. Lett. B **562**, 147 (2003);

S. Nojiri, S.D. Odintsov, Phys. Lett. B **565**, 1 (2003);

F. de. Paolis, M. Jamil, A. Qadir,Int. J. Theor. Phys. **49**, 621,2010;

M. Jamil, Munner. A. Rashid, Eur. Phys. J. C. **58**, 111-114,2008;

M. Jamil, Eur. Phys. J. C. **62**, 609-614,2009;

M. Jamil, Int. J. Theor. Phys. **49**, 144-151,2010.

[8] E. Elizalde, S. Nojiri, S.D. Odinstov, Phys. Rev. D **70**, 043539 (2004);

S. Nojiri, S.D. Odintsov, S. Tsujikawa, Phys. Rev. D **71**, 063004 (2005);

A. Anisimov, E. Babichev, A. Vikman, J. Cosmol. Astropart. Phys. **06**, 006 (2005).

[9] T. Chiba, T. Okabe, M. Yamaguchi, Phys. Rev. D **62**, 023511(2000);

C. Armendariz-Picon, V. Mukhanov, P.J. Steinhardt, Phys. Rev. Lett. **85**, 4438 (2000);

C. Armendariz-Picon, V. Mukhanov, P.J. Steinhardt, Phys. Rev. D **63**, 103510 (2001).

[10] A. Sen, J. High Energy Phys. **04**, 048 (2002);

T. Padmanabhan, Phys. Rev. D **66**, 021301 (2002);

T. Padmanabhan, T.R. Choudhury, Phys. Rev. D **66**, 081301 (2002).

[11] M. Gasperini, F. Piazza, G. Veneziano, Phys. Rev. D **65**, 023508 (2002); N. Arkani-Hamed, P. Creminelli, S. Mukohyama, M. Zaldarriaga, J. Cosmol. Astropart. Phys. **04**, 001 (2004); F. Piazza, S. Tsujikawa, J. Cosmol. Astropart. Phys. **07**, 004 (2004).

[12] A. Kamenshchik, U. Moschella, V. Pasquier, Phys. Lett. B **511**, 265 (2001); M. C. Bento, O. Bertolami, A. A. Sen, Phys. Rev. D **66**, 043507 (2002);

[13] M. R. Setare, Eur. Phys. J. C **52**, 689, 2007.

[14] C. Deffayet, G. R. Dvali, G. Gabadaaze, Phys. Rev. D **65**, 044023 (2002); V. Sahni, Y. Shtanov, J. Cosmol. Astropart. Phys. **0311**, 014 (2003).

[15] P. Horava, D. Minic, Phys. Rev. Lett. **85**, 1610 (2000); P. Horava, D. Minic, Phys. Rev. Lett. **509**, 138 (2001); S. Thomas, Phys. Rev. Lett. **89**, 081301 (2002); M. R. Setare, Phys. Lett. B **644**, 99, 2007; M. R. Setare, Phys. Lett. B **654**, 1, 2007; M. R. Setare, Phys. Lett. B **642**, 1, 2006; M. R. Setare, Eur. Phys. J. C **50**, 991, 2007; M. R. Setare, Phys. Lett. B **648**, 329, 2007; M. R. Setare, Phys. Lett. B **653**, 116, 2007.

[16] R.G. Cai, Phys. Lett. B **657**, (2007) 228; H. Wei, R.G. Cai, Phys. Lett. B **660**, 113 (2008).

[17] Jamil, M., Munner, A. Rashid, Eur. Phys. J. C **56**, 429-434, 2008;
Jamil, M., Rahman, F., ; Eur. Phys. J. C **64**, 97-105, 2009;
Farooq, M. Umar, Jamil, M., Munner, A. Rashid, Int. J. Theor. Phys. **49**, 2278-2287, 2010;
Jamil, M., Saridakis, E. N., JCAP **1007**, 028, 2010;
Sadjadi, H. M., Jamil, M., Gen. Rel. Grav. **43**, 1759-1775, 2011.

[18] G. t Hooft, gr-qc/9310026; L. Susskind, J. Math. Phys. **36**, 6377 (1995).

[19] F. Karolyhazy, Nuovo.Cim. A **42** (1966) 390; F. Karolyhazy, A. Frenkel and B. Lukacs, in Physics as natural Philosophy edited by A. Shimony and H. Feschbach, MIT Press, Cambridge, MA, (1982); F. Karolyhazy, A. Frenkel and B. Lukacs, in Quantum Concepts in Space and Time edited by R. Penrose and C.J. Isham, Clarendon Press, Oxford, (1986).

[20] O. Bertolami, F. Gil Pedro, M. Le Delliou, Phys. Lett. B **654**, 165 (2007).

[21] C. Feng, B. Wang, Y. Gong, R.K. Su, JCAP **0709**, 005 (2007).

[22] J. Christensen-Dalsgard, *Lecture Notes on Stellar Structure and Evolution, 6th edn.* (Aarhus University Press, Aarhus, 2004).

[23] U. Mukhopadhyay and S. Ray, Mod. Phys. Lett. A **23**, 3198,2008.

[24] K. Karami, A. Abdolmaleki, Astrophys. Space Sci.**330**, 133,2010.

[25] K. Karami, S. Ghaffari, J. Fehri, Eur. Phys. J. C, **64**, 85 (2009).

[26] K. Karami, A. Abdolmaleki, arXiv:1009.3587.

[27] M. Malekjani, A. Khodam-Mohammadi, M. Taji, Int. J. Theor. Phys. 50, 312, 2011.

[28] S. Nojiri, S. D. Odintsov, S. Tsujikawa, Phys. Rev. D **71**, 063004 (2005).

[29] Sahni, V., Saini, T.D., Starobinsky, A.A., Alam, U.: JETP Lett. 77, 201 (2003).

[30] Alam, U., Sahni, V., Saini, T.D., Starobinsky, A.A.: Mon. Not. R. Astron. Soc. 344, 1057 (2003a).

[31] Zimdahl, W., Pavon, D.: Gen. Relativ. Gravit. 36, 1483 (2004).

[32] Zhang, X.: Phys. Lett. B 611, 1 (2005a).

[33] Zhang, X.: Int. J. Mod. Phys. D 14, 1597 (2005b).

[34] Zhang, J., Zhang, X., Liu, H.: arXiv:0705.4145 [astro-ph] (2007).

[35] Setare, M.R., Zhang, J., Zhang, X.: J. Cosmol. Astropart. Phys. 0703, 007 (2007).

[36] Chang, B.R., Liu, H.Y., Xu, L.X., Zhang, C.W., Ping, Y.L.: J. Cosmol. Astropart. Phys. 0701, 016 (2007).

[37] Shao, Y., Gui, Y.: gr-qc/0703111.

[38] Malekjani, M., Khodam-Mohammadi, A. and N. Nazari-Pooya, Astrophys Space Sci, 334:193201, 2011.

[39] Zhang, L., Cui, J., Zhang, J., Zhang, X.: Int. J. Mod. Phys. D 19,21 (2010)

[40] Khodam-Mohammadi, A., Malekjani, M.: Astrophys. Space Sci. 331, 265 (2010).

[41] Wei, H., Cai, R.G.: Phys. Lett. B 655, 1 (2007)

[42] Malekjani, M., Khodam-Mohammadi, A.: Int. J. Mod. Phys. D 19,1 (2010).

[43] Jamil, M., Debnath, U., Int. J. Theor. Phys. **50**, 1602-1613,2011;
Jamil, M., Int. J. Theor. Phys. **49**, 2829,2010;
Setare, M. R., Jamil, M., Gen. Relativ. Gravit. **43**, 293-303, 2011;
Debnath, U., Jamil, M., Astrophys. Space Sci. **335**, 545-552, 2011;
Jamil, M., Debnath, U., Astrophys. Space Sci. **333**, 3, 2011.

[44] Scherrer, R.J.: Phys. Rev. D 73, 043502 (2006)

[45] Chiba, T.: Phys. Rev. D 73, 063501 (2006)

[46] Barger, V., Guarnaccia, E., Marfatia, D.: Phys. Lett. B 635, 61 (2006)

[47] Zhao,W.:Phys.Rev.D 73, 123509 (2006)

[48] Zhao, W.: Phys. Lett. B 655, 97 (2007)

[49] Calcagni, G., Liddle, A.R.: Phys. Rev. D 74, 043528 (2006)

[50] Guo, Z.K., Piao, Y.S., Zhang, X.M., Zhang, Y.Z.: Phys. Rev. D 74, 127304 (2006)

[51] Huang, Z.G., Li, X.H., Sun, Q.Q.: Astrophys. Space Sci. 310,53 (2007a)

[52] Huang, Z.G., Lu, H.Q., Fang, W.: Int. J. Mod. Phys. D 16, 1109 (2007b)

[53] de Putter, R., Linder, E.V.: Astropart. Phys. 28, 263 (2007)

[54] A. Sheykhi, Phys. Lett. B **680**, 113 (2009); H. Wei & R. G. Cai, Phys. Lett. B **660**, 113 (2008); L. Zhang, J. Cui, J. Zhang & X. Zhang, Int. J. Mod. Phys. D **19**, 21 (2010).

[55] L. P. Chimento, Phys. Rev. D **81**, 043525 (2010).

[56] Malekjani. M., Khodam-Mohammadi. A., Nazari-Pooya, N., Astrophys Space Sci (2011) 332: 515524.